

# Solid-State High-Resolution $^1\text{H}$ and $^2\text{D}$ NMR Study of the Electron Spin Density Distribution of the Hydrogen-Bonded Organic Ferromagnetic Compound 4-Hydroxyimino-TEMPO

Goro Maruta,<sup>1a</sup> Sadamu Takeda,<sup>\*1b,c</sup> Ron Imachi,<sup>1d</sup> Takayuki Ishida,<sup>1d</sup> Takashi Nogami,<sup>1c,d</sup> and Kizashi Yamaguchi<sup>1a</sup>

Contribution from the Department of Chemistry, Graduate School of Science, Osaka University, Toyonaka, Osaka 560-0043, Japan, Department of Chemistry, Faculty of Engineering, Gunma University, Kiryu, Gunma 376-8515, Japan, Institute for Molecular Science, Myodaiji, Okazaki 444-8585, Japan, and Department of Applied Physics and Chemistry, The University of Electro-Communications, Chofu, Tokyo 182-8585, Japan

Received July 7, 1998. Revised Manuscript Received November 5, 1998

**Abstract:** The electron spin density distribution at hydrogen atoms of 4-hydroxyimino-2,2,6,6-tetramethylpiperidin-1-yloxy (4-hydroxyimino-TEMPO), which has recently been shown to act as a molecular ferromagnet at low temperature, was determined in the crystalline phase on the basis of the temperature dependence of the Fermi contact shifts in the magic angle spinning deuterium NMR spectrum to elucidate the mechanism of intermolecular magnetic interaction. There are two kinds of close contacts among neighboring radical molecules in the crystalline phase. An axial methyl hydrogen atom locates near a neighboring N–O radical group, and the hydroxyl group undergoes hydrogen bonding with another neighboring N–O radical group. The plus and minus signs of the observed hyperfine coupling constants  $A_D$  of methyl deuteriums indicate that there are two different mechanisms for the electron spin density distribution. Equatorial  $\text{CD}_3$  groups show negative coupling constants ( $A_D = -0.24$  MHz) induced by an intramolecular spin polarization mechanism, whereas the positive hyperfine coupling constants ( $A_D = +0.12$  MHz) of axial  $\text{CD}_3$  groups indicate that a single occupied MO spreads out partly toward the axial  $\text{CD}_3$  groups by hyperconjugation. The small positive hyperfine coupling constant of the axial methyl group is due to averaging of the one positive and two negative values of the three deuterium atoms of the methyl group caused by rapid rotation. The intermolecular magnetic interaction through the axial methyl group seems to be sensitive to the orientation of the methyl group and can be ferromagnetic in a crystal of 4-hydroxyimino-TEMPO. The large negative hyperfine coupling constant ( $A_D = -0.45$  MHz) observed for the NOD group strongly implies that hydrogen bonding mediates the intermolecular magnetic interaction in the crystalline phase. The present experimental results and molecular orbital calculations indicate that ferromagnetic interaction exists in the hydrogen-bonded chains running along the crystallographic  $c$  axis, and that the two chains can be considered to be coupled ferromagnetically through the axial methyl groups to form a double chain. In the directions of the crystallographic  $a$  and  $b$  axes, weak ferromagnetic interactions are expected on the basis of the measured spin density distributions of the deuterium atoms of the equatorial methyl and the methylene groups which participate in interchain contacts in the crystallographic  $a$ – $b$  plane. The  $^1\text{H}$  and  $^2\text{D}$  NMR spectra measured for solutions demonstrated that the spin density distribution of the radical molecule changes dramatically between the solution and crystalline phases.

## 1. Introduction

Organic ferromagnetism is one of the realizations of tremendous potential of organic compounds. Molecules that exhibit this feature can be designed to exhibit a variety of functions by chemical modifications and have attracted the interest of chemists in a wide range of fields, such as organic, physical, and theoretical chemistry. Ferromagnetism in purely organic materials has been a subject of great interest ever since Kinoshita et al. found a molecular ferromagnet at low temperature in 1991.<sup>2</sup> Most organic ferromagnetic crystals are based on

nitroxide (N–O) radicals.<sup>3–7</sup> A main interest in this field is to be able to control intermolecular magnetic interaction in the solid state to produce ferromagnetic ordering. Considerable effort has been made to realize ferromagnetic ordering through the synthesis of a variety of derivatives of the nitroxide radical species, since the electron spin density distribution in a radical molecule and the molecular arrangement in the crystalline phase are believed to be controlled by chemical modifications of the

\* Address correspondence to this author at Department of Chemistry, Faculty of Engineering, Gunma University, Kiryu, Gunma 376-8515, Japan. Tel.: (+81)277301382. Fax: (+81)277301380. E-mail: stakeda@chem.gunma-u.ac.jp.

(1) (a) Osaka University. (b) Gunma University. (c) Institute for Molecular Science. (d) The University of Electro-Communications.

(2) Kinoshita, M.; Turek, P.; Tamura, M.; Nozawa, K.; Shiomi, D.; Nakazawa, Y.; Ishikawa, M.; Takahashi, M.; Awaga, K.; Inabe T.; Maruyama, Y. *Chem. Lett.* **1991**, 1225–1228.

(3) Chiarelli, R.; Novak, M.; A.; Rassat, A.; Tholence, J. L. *Nature* **1993**, 363, 147–149.

(4) Nogami, T.; Tomioka, K.; Ishida, T.; Yoshikawa, H.; Yasui, M.; Iwasaki, F.; Iwamura, H.; Takeda N.; Ishikawa, M. *Chem. Lett.* **1994**, 29–32.

(5) Sugawara, T.; Matsushita, M. M.; Izuoka, A.; Wada, N.; Takeda N.; Ishikawa, M. *J. Chem. Soc., Chem. Commun.* **1994**, 1723–1724.

(6) Cirujeda, J.; Mas, M.; Molins, E.; Panthou, F. L.; Laugier, J.; Park, J. G.; Paulsen, C.; Rey, P.; Rovira, C.; Veciana, J. *J. Chem. Soc., Chem. Commun.* **1995**, 709–710.

(7) Sugimoto, T.; Tsujii, M.; Suga, T.; Hosoi, N.; Ishikawa, M.; Takeda N.; Shiro, M. *Mol. Cryst. Liq. Cryst.* **1995**, 272, 183–194.

molecules to give intermolecular ferromagnetic ordering. The magnitude and sign of the electron spin density distribution in a radical molecule are some of the basic properties for discussing intermolecular magnetic interactions. The alternation of the positive and negative electron spin density is brought about by an intramolecular spin polarization effect through chemical bonds even for atoms away from the N–O radical site.<sup>8,9</sup> A hyperconjugation effect may also be expected for atoms close to the N–O radical site in the same molecule, and this effect is very sensitive to the molecular geometry.<sup>10</sup> For intermolecular magnetic interactions in the crystalline phase, at least two types of ferromagnetic interactions can be theorized, i.e., (1) a direct interaction between the single occupied molecular orbitals (SOMOs) of neighboring N–O radical groups and (2) indirect interactions between distant N–O radical groups through a spin-polarized network including nonbonded intermolecular atom contacts.<sup>11–14</sup> The direct SOMO–SOMO interaction depends sensitively on the mutual direction and distance between the two neighboring N–O radicals. Only a limited configuration, i.e., no overlap integral for the SOMO–SOMO interaction, may give ferromagnetic interaction; otherwise, antiferromagnetic interaction occurs.<sup>15</sup> It is difficult to design materials in which ferromagnetic ordering through successive SOMO–SOMO coupling is realized. On the other hand, it is easier to achieve indirect intermolecular ferromagnetic coupling among molecules in the crystalline phase. Ferromagnetic interaction can occur when atoms bearing a negative electron spin density are in close contact with the N–O radical group of a neighboring molecule. For most nitroxide radical molecules, particularly 2,2,6,6-tetramethylpiperidin-1-yloxy (TEMPO) derivatives, the N–O radical group is protected from chemical reaction by methyl groups through steric hindrance. By X-ray structure analysis, it has often been found for TEMPO derivatives that methyl hydrogens are in close contact with an adjacent N–O radical group in the crystalline phase. Such hydrogen atoms are expected to be intermolecular ferromagnetic exchange couplers on the basis of the crystal structure.<sup>16,17</sup>

Crystalline 4-hydroxyimino-2,2,6,6-tetramethylpiperidin-1-yloxy (4-hydroxyimino-TEMPO) has been found to exhibit a ferromagnetic phase transition at low temperature ( $T_c \approx 0.25$  K).<sup>16</sup> In this crystal, the hydroxyl group is linked to an adjacent N–O radical group by a hydrogen bond to form an infinite chain along the  $c$  axis of the crystal, and successive zigzag contacts exist between methyl hydrogens and N–O radical groups in different chains,<sup>18</sup> as depicted in Figure 1. It would be useful to determine what kind of intermolecular contact serves as the ferromagnetic interaction in this crystal to establish a principle for producing ferromagnetic ordering in the crystalline phase

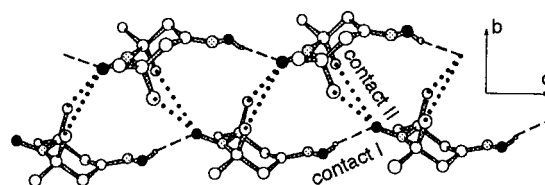


**Figure 1.** Crystal structure of 4-hydroxyimino-TEMPO determined by an X-ray diffraction experiment.<sup>18</sup> There are two kinds of close contacts, i.e., hydrogen bonding between a hydroxyl hydrogen and an adjacent N–O radical group (contact I) and axial methyl contact with a neighboring N–O radical group (contact II). The O···O distance for contact I is 0.275 nm, and the C···O distances for contact II are 0.333 and 0.373 nm. The static disorder of the hydroxyl group into two crystallographically equivalent sites is not depicted for simplicity. Hydrogen atoms not in the hydroxyl group are also omitted.

of organic magnetic compounds and to understand the characteristics and functions of open-cell molecules.

In this paper, we report our results for the experimental determination of the isotropic hyperfine coupling constants between nuclear and electron spins for 4-hydroxyimino-TEMPO in the crystalline phase. High-speed magic angle spinning <sup>1</sup>H and <sup>2</sup>D NMR spectra were measured for the crystalline phase. The <sup>1</sup>H NMR spectrum gave poor resolution compared to the <sup>2</sup>D NMR spectrum due to rapid spin diffusion among the proton nuclear spins. Our results showed that the magic angle spinning <sup>2</sup>D NMR technique is an excellent method for studying the electron spin density distribution of organic radical crystals. The <sup>1</sup>H and <sup>2</sup>D NMR spectra were also measured for solutions to demonstrate that the spin density distribution of the radical molecule changes dramatically between the solution and crystalline phases. The hyperfine coupling constants were determined for a series of partially deuterated specimens on the basis of the temperature dependence of the Fermi contact shifts as measured by magic angle spinning deuterium nuclear magnetic resonance (<sup>2</sup>D-MAS NMR). The experimentally determined electron spin density distribution in the crystalline phase was compared with theoretical calculations based on the density functional theory, and the magnetic interaction path in the crystalline phase is discussed.

## 2. Method

The static <sup>2</sup>D NMR spectrum of a paramagnetic polycrystalline specimen exhibits a broad width with fine structure due to quadrupole interaction of deuterons and dipole interaction between the nuclear and electron spins. The magic angle spinning (MAS) technique averages the two interactions in principle and provides the isotropic shift of the <sup>2</sup>D NMR absorption line. The observed isotropic shift on a ppm scale consists of the Fermi contact term, the pseudo contact term, and the temperature-independent diamagnetic term, as follows:

$$\delta_{\text{iso}} = \delta_{\text{Fermi}} + \delta_{\text{pseudo}} + \delta_{\text{dia}} \quad (1)$$

$$\delta_{\text{Fermi}} = \frac{\mu_B}{3k_B T} \frac{A_{\text{Fermi}}}{\gamma_D/2\pi} \left( \frac{g_{xx} + g_{yy} + g_{zz}}{3} \right) S(S+1)F \quad (2)$$

$$\delta_{\text{pseudo}} = \frac{\mu_B^2}{18k_B T r^3} \{ [2g_{zz}^2 - (g_{xx}^2 + g_{yy}^2)] (3 \cos^2 \theta - 1) - 3(g_{yy}^2 - g_{xx}^2) \sin^2 \theta \cos 2\Omega \} S(S+1)F \quad (3)$$

where  $A_{\text{Fermi}}$  is the Fermi contact coupling constant of the nucleus D in hertz,  $T$  is the absolute temperature,  $F$  represents the intermolecular exchange interaction,  $r$  is the length of a vector  $\mathbf{r}$  from the unpaired electron to the nucleus,  $\theta$  and  $\Omega$  are the polar angles of the vector with respect to the principal axes of a  $g$ -value, and the other terms have their usual meanings.<sup>19,20</sup> The anisotropy of the  $g$ -value is very

(8) McConnell H. M.; Chesnut, D. B. *J. Chem. Phys.* **1957**, *27*, 984–985.

(9) Yamanaka, S.; Kawakami, T.; Yamada, S.; Nagao, H.; Nakano, M.; Yamaguchi, K. *Chem. Phys. Lett.* **1995**, *240*, 268–277.

(10) Heller, C.; McConnell H. M. *J. Chem. Phys.* **1960**, *32*, 1535–1539.

(11) McConnell, H. M. *J. Chem. Phys.* **1963**, *39*, 1910–1910.

(12) Yamaguchi, K.; Fueno, T.; Nakasuji, K.; Murata, I. *Chem. Lett.* **1986**, 629–632.

(13) Awaga, K.; Sugano, T.; Kinoshita, M. *Chem. Phys. Lett.* **1987**, *141*, 540–544.

(14) Yamaguchi, K.; Fueno, T. *Chem. Phys. Lett.* **1989**, *159*, 465–471.

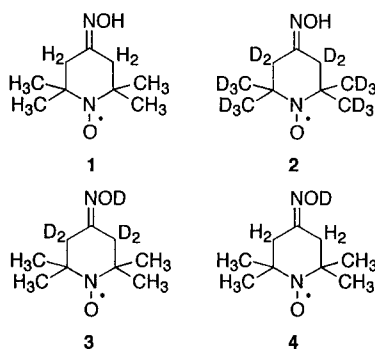
(15) Kawakami, T.; Oda, A.; Mori, W.; Yamaguchi, K.; Inoue, K.; Iwamura, H. *Mol. Cryst. Liq. Cryst.* **1996**, *279*, 29–38.

(16) Nogami, T.; Ishida, T.; Yasui, M.; Iwasaki, F.; Iwamura, H. Takeda N.; Ishikawa, M. *Mol. Cryst. Liq. Cryst.* **1996**, *279*, 97–106.

(17) Nogami, T.; Ishida, T.; Yasui, M.; Iwasaki, F.; Takeda, N.; Ishikawa, M.; Kawakami T.; Yamaguchi, K. *Bull. Chem. Soc. Jpn.* **1996**, *69*, 1841–1848.

(18) Bordeaux, P. D.; Lajz rowicz, J. *Acta Crystallogr.* **1977**, *B33*, 1837–1840.

Chart 1



small for typical organic radical crystals; e.g., the anisotropy of the  $g$ -value of the TEMPO radical falls in the range  $2.00620 \pm 0.0040$ .<sup>21</sup> Thus, in our case, the contribution of the pseudo contact term is estimated to be less than 0.01 MHz for  $r = 1.8 \text{ \AA}$ , and the pseudo contact term ( $\delta_{\text{pseudo}}$ ) can be neglected in comparison with the Fermi contact term to determine the hyperfine coupling constant  $A_D (=A_{\text{Fermi}})$ . Since the estimated exchange interaction among the molecules is much smaller than the thermal energy above 194 K,<sup>16</sup> the term  $F$  in eqs 2 and 3 becomes unity, and the hyperfine coupling constant  $A_D$  can be directly determined from the slope of the temperature dependence of the observed isotropic shift in the <sup>2</sup>D-MAS NMR spectrum. The observed coupling constant  $A_D$  is related to the electron spin density  $\rho(R_D)$  at the nuclear position  $R_D$  as follows:<sup>19</sup>

$$A_D = A_{\text{Fermi}} = \frac{8\pi}{3} g\mu_B \frac{\gamma_D}{2\pi} \rho(R_D) \quad (4)$$

### 3. Experimental Section

4-Hydroxyimino-TEMPO (1) and its partially deuterated analogues 2–4 (Chart 1) were prepared as reported previously.<sup>22</sup> The selective methylene deuteration of 4-oxo-TEMPO was achieved by a proton–deuteron exchange reaction of the enolate anion in a basic D<sub>2</sub>O solution. The crystal structure of the present specimen as determined by single-crystal X-ray diffraction<sup>23</sup> was in agreement with that reported previously.<sup>18</sup> Pulverized specimens were evacuated under  $10^{-3}$  mmHg for several hours to remove the solvent which was used for recrystallization. The solvent that had adsorbed to the powder sample was difficult to completely remove, and small sharp signals of the solvent without a spinning sideband were detected by the MAS NMR measurement.

<sup>2</sup>D-MAS NMR spectra of 2–4 were measured by using a single pulse method at a resonance frequency of 46.1 MHz with a Bruker DSX300 spectrometer and a 4-mm CP/MAS probe between 190 and 300 K. The  $\pi/2$  pulse length was 1.2  $\mu\text{s}$ . A conventional zirconia rotor (4 mm) with a boron nitride cap was used. The specimen (ca. 10–20 mg) was carefully packed at the center of the rotor (2–3 mm long) to achieve a homogeneous temperature at the sample position, and Teflon powder was used as a spacer. Dry N<sub>2</sub> gas that evaporated from the liquid N<sub>2</sub> container was used for the high-speed magic angle spinning (7–10 kHz).

<sup>1</sup>H-MAS NMR spectra of 1 and 2 were measured by a similar method with a resonance frequency of 300.13 MHz and at a higher spinning rate (9–15 kHz).

The thermometer of the MAS probe was calibrated against the isotropic chemical shift of the <sup>207</sup>Pb-MAS NMR spectrum of Pb(NO<sub>3</sub>)<sub>2</sub>.<sup>24</sup>

(19) McConnell, H. M.; Chesnut, D. B. *J. Chem. Phys.* **1958**, *28*, 107–117.

(20) Kurland, R. J.; McGarvey, B. R. *J. Magn. Reson.* **1970**, *2*, 286–301.

(21) Bordeaux, D.; Lajzerowicz-Bonneteau, J.; Briere, R.; Lemaire H.; Rasset, A. *Org. Magn. Reson.* **1973**, *5*, 47–52.

(22) Imachi, R.; Ishida, T.; Nogami, T.; Yasui, M.; Iwasaki, F.; Takeda N.; Ishikawa, M. *Synth. Met.* **1997**, *85*, 1743–1744.

(23) Iwasaki, F.; Yasui, M. Unpublished work.

(24) Bielecki A.; Burum, D. P. *J. Magn. Reson.* **1995**, *A116*, 215–220.

and the solid–solid phase transition temperatures<sup>25</sup> of cyclooctanone (C<sub>8</sub>H<sub>14</sub>O,  $T_1 = 227 \text{ K}$ ) and diazabicyclooctane ((C<sub>2</sub>H<sub>4</sub>)<sub>3</sub>N<sub>2</sub>,  $T_1 = 350 \text{ K}$ ), which were detected by <sup>1</sup>H-MAS NMR at spinning rates of 3.5 and 10 kHz. These brittle plastic phase transition temperatures of orientationally disordered crystals (ODCs) were determined by a differential thermal analysis. Pulverized crystals of Pb(NO<sub>3</sub>)<sub>2</sub> and one of the ODCs were packed into the same rotor, and <sup>207</sup>Pb-MAS NMR and <sup>1</sup>H-MAS NMR spectra were measured alternately under the same conditions with a double-tuned MAS NMR probe for precise calibration of the temperature. The resulting temperature coefficient of the isotropic chemical shift of <sup>207</sup>Pb 0.784 ppm/K was almost the same as that reported in ref 24 (0.753 ppm/K). The increase in the temperature of the specimen with an increase in the spinning rate was also examined and calibrated. The brittle plastic phase transition temperatures of ODCs are convenient to use as a temperature reference, since solid materials can be easily put into the rotor together with Pb(NO<sub>3</sub>)<sub>2</sub>. The uncertainty of the temperature measurement after the calibration was 4 K, and the temperature fluctuation during the accumulation was within 1 K. All <sup>2</sup>D NMR shifts were measured from an external second reference of acetone-*d*<sub>6</sub> (2.05 ppm), and all <sup>1</sup>H NMR shifts were measured from tetramethylsilane dissolved in CCl<sub>4</sub>.

### 4. Theoretical Calculations

The electron spin density at position  $R$  can be computed as the difference between the electron density of  $\alpha$ -spin and that of  $\beta$ -spin,<sup>19</sup>

$$\rho(R) = \sum_i^{\text{occ}} |\psi_i^\alpha(R)|^2 - \sum_i^{\text{occ}} |\psi_i^\beta(R)|^2 \quad (5)$$

where  $\psi_i^\alpha$  is an unrestricted molecular orbital for the  $\alpha$ -spin electron and each summation runs over occupied orbitals.

An effective exchange integral  $J$  of a radical pair can be estimated from the energy difference between the triplet (high-spin) and singlet (low-spin) states,<sup>26,27</sup>

$$J = \frac{{}^{\text{LS}}E - {}^{\text{HS}}E}{{}^{\text{HS}}\langle S^2 \rangle - {}^{\text{LS}}\langle S^2 \rangle} \quad (6)$$

where  ${}^{\text{HS}}\langle S^2 \rangle$  and  ${}^{\text{HS}}E$  are respectively the expectation value of  $S^2$  and the energy of the high-spin state based on unrestricted wave functions.

Using the GAUSSIAN 94 software package,<sup>28</sup> we performed BLYP/6-31G(d,p) and B3LYP/6-31G(d,p) calculations on an isolated molecule, on a hydrogen-bonded dimer, and on a methyl-contacted dimer. The coupling constant  $A_D$  between deuterium spin and electron spin, and the effective exchange integral  $J$ , were obtained using eqs 4–6. INDO calculations were also performed. The geometric structures of the molecule and of the dimers were taken from the crystal structure,<sup>18</sup> except for the hydroxyl hydrogen atom. The position of the hydrogen atom of the trimer that is composed of contact I and contact II in Figure 1, since the position of the hydroxyl hydrogen atom was not precisely determined by X-ray diffraction due to static disorder of the molecule in the crystalline phase.<sup>18</sup>

### 5. Results and Discussion

**Advantages of Deuterium MAS NMR for Organic Magnetic Solids.** Figure 2 shows the <sup>1</sup>H-MAS NMR spectrum (a)

(25) Chezeau, J. M.; Strange, J. H. *Phys. Rep.* **1979**, *53*, 1–92.

(26) Maruta, G.; Yamaki, D.; Mori, W.; Yamaguchi K.; Nishide, H. *Mol. Cryst. Liq. Cryst.* **1996**, *279*, 19–28.

(27) Yamaguchi, K.; Fukui, H.; Fueno, T. *Chem. Lett.* **1986**, 625–628

(28) Frisch, M. J.; Trucks, G. W.; Schlegel, H. B.; Gill, P. M. W.; Johnson, B. G.; Robb, M. A.; Cheeseman, J. R.; Keith, T.; Petersson, G. A.; Montgomery, J. A.; Raghavachari, K.; Al-Laham, M. A.; Zakrzewski, V. G.; Ortiz, J. V.; Foresman, J. B.; Cioslowski, J.; Stefanov, B. B.; Nanayakkara, A.; Challacombe, M.; Peng, C. Y.; Ayala, P. Y.; Chen, W.; Wong, M. W.; Andres, J. L.; Replogle, E. S.; Gomperts, R.; Martin, R. L.; Fox, D. J.; Binkley, J. S.; Defrees, D. J.; Baker, J.; Stewart, J. P.; Head-Gordon, M.; Gonzalez, C.; Pople, J. A. *Gaussian 94*; Gaussian, Inc.: Pittsburgh, PA, 1995.

(29) Stewart, J. J. P. *J. Comput. Chem.* **1989**, *10*, 209–220.

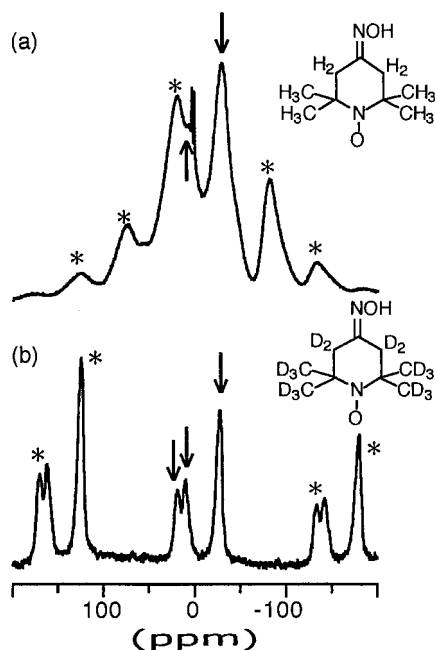


**Figure 2.** (a)  $^1\text{H}$ -MAS NMR spectrum of **1** measured at a spinning rate of 15 kHz at 310 K. Sharp signals near 3 ppm are due to a very small amount of ethanol adsorbed by the powder specimen. (b)  $^2\text{D}$ -MAS NMR spectrum of **2** measured at a spinning rate of 7 kHz at 298 K. Arrows indicate the isotropic shifts, and asterisks represent spinning sidebands.

of the fully protonated specimen **1** and the  $^2\text{D}$ -MAS NMR spectrum (b) of the methyl and methylene deuterated analogue **2**, which were measured at room temperature at spinning rates of 15 and 7 kHz, respectively. The spinning sidebands were clearly distinguished by using several different spinning speeds. For the  $^1\text{H}$ -MAS NMR spectrum, only the two signals indicated by arrows were poorly resolved, i.e., the shoulder at +8 ppm and the peak at -28 ppm. On the other hand, three peaks were clearly resolved, and they were located far from the spinning sidebands in the  $^2\text{D}$ -MAS NMR spectrum. All three peaks were assigned to the methyl groups. The absorption lines of the methylene groups overlapped the peak of the methyl groups at -28 ppm, as discussed below. The advantage of the  $^2\text{D}$ -MAS NMR spectrum for organic magnetic solids is based on the small magnetogyric ratio  $\gamma_{\text{D}}$  of deuterium compared to that ( $\gamma_{\text{H}}$ ) of a proton ( $\gamma_{\text{D}}/\gamma_{\text{H}} = 0.15$ ), as in solutions.<sup>30</sup> The internuclear dipole coupling is small for deuterium, and magic angle spinning is more efficient due to the slower spin diffusion than in the case of a proton. The dipole coupling measured in hertz between deuterium and an electron spin is also small, and the line width of the isotropic shift is smaller than that in the case of a proton. The hydroxyl deuterium of **4** was clearly detected by  $^2\text{D}$ -MAS NMR, while the hydroxyl proton of **2** was not observed by  $^1\text{H}$ -MAS NMR. Measurement of the Fermi contact shift of the hydroxyl deuterium is important for discussing magnetic interaction through hydrogen bonding in the crystalline phase.

To determine the hyperfine coupling constant and the electron spin density distribution of each atom of organic radical molecules, a variety of experimental techniques have been used, such as NMR,<sup>31</sup> ESR,<sup>32,33</sup> and polarized neutron diffraction.<sup>34</sup> The techniques of NMR and ESR have been applied mostly to

solutions, and few experiments have been performed for the crystalline phase. For example, wide-line proton NMR was used to estimate the hyperfine coupling constant of protons of TEMPO derivatives.<sup>35,36</sup> However, the resolution of the spectrum is not sufficient for powder samples. The polarized neutron diffraction technique is a powerful tool for determining the electron spin density distribution in the crystalline phase, particularly for atoms with a large electron spin density such as N, O, and C. On the other hand,  $^2\text{D}$ -MAS NMR is very sensitive to the electron spin density of hydrogen atoms, which are expected to play an important role in magnetic interaction in organic magnetic materials.

In addition to the advantage of  $^2\text{D}$ -MAS NMR described above, partial deuteration enabled us to obtain a simple spectrum and to assign the peaks very easily, as described below.

**Different Hyperfine Coupling Constants of 4-Hydroxyimino-TEMPO in Solution and in the Crystalline Phase.** The isotropic shifts of 4-hydroxyimino-TEMPO depended on its environment, such as in methanol solution and in the crystalline phase, as demonstrated in Figure 3. Two peaks were resolved for both the methylene (a) and methyl (c) groups even in solution, suggesting that interconversion between the axial and equatorial positions due to ring puckering is very slow at 298 K. The isotropic shifts of the methyl and methylene groups in the crystalline phase changed dramatically from those in the methanol solution. This result suggests that the electron spin density distribution changes sensitively with deformation of the molecule. Since the molecular geometry may be different between the solution and crystalline phases, the hyperfine coupling constant should be determined in the crystalline phase of interest to discuss the mechanism of the intermolecular magnetic interaction.

The sharp signals which appeared in spectrum c are due to protonated solvent in  $\text{CD}_3\text{OD}$ . The solvent  $\text{CD}_3\text{OD}$  shows a strong signal near 5 ppm in spectrum b. The integrated intensity of the solvent is much smaller than that of specimen **3**, since the polycrystalline specimen showed numerous spinning sidebands while the solvent exhibited none.

**Determination of Hyperfine Coupling Constants in the Crystalline Phase.** Temperature-dependent variations of the  $^2\text{D}$ -MAS NMR spectra of (a) the methylene groups of **3**, (b) the methyl groups of **2**, and (c) the hydroxyl group of **4** are summarized in Figure 4. Many spinning sidebands appeared over the frequency region of the static  $^2\text{D}$  NMR line width, and only the isotropically shifted region is shown for respective partially deuterated compounds. Before discussing the hyperfine coupling constants of deuterium atoms, we should mention the motion of the methyl groups. Based on the measurement of the static  $^2\text{D}$  NMR line shape of **2** above 130 K, all of the methyl groups apparently rotate rapidly around their own  $\text{C}_3$  axis, while the methylene groups remain static. The observed intensity of the isotropically shifted signal of the methylene group is much smaller than that of the methyl group, since the signal intensity is distributed over the spinning sidebands and the static line width of a methylene group is much larger than that of a rotating methyl group.

(32) Aurich, H. G. Nitroxides. In *Nitrones, Nitronates and Nitroxides*; Patai, S., Rappoport, Z., Eds.; John Wiley & Sons: Chichester, 1989; pp 335–338.

(33) Takui, T.; Miura, Y.; Inui, K.; Teki, Y.; Inoue, M.; Itoh, K. *Mol. Cryst. Liq. Cryst.* **1995**, *271*, 55–66.

(34) Zheludev, A.; Barone, V.; Bonnet, M.; Delly, B.; Grand, A.; Ressouche, E.; Rey, P.; Subra, R.; Schweizer, J. *J. Am. Chem. Soc.* **1994**, *116*, 2019–2027.

(35) Ondercin, D.; Sandreczki, T.; Kreilick, R. W. *J. Magn. Reson.* **1979**, *34*, 151–169.

(36) Ferrieu, F.; Nechtschein, M. *Chem. Phys. Lett.* **1971**, *11*, 46–51.

(30) Johnson, A.; Everett, G. W., Jr. *J. Am. Chem. Soc.* **1970**, *92*, 6705–6706

(31) Kreilick, R. W. NMR Studies of Organic Radicals. In *NMR of Paramagnetic Molecules*; Mar, G. N. L., Horrocks, W. D., Jr., Holm, R. H., Eds.; Academic Press: New York, 1973; pp 604–618.

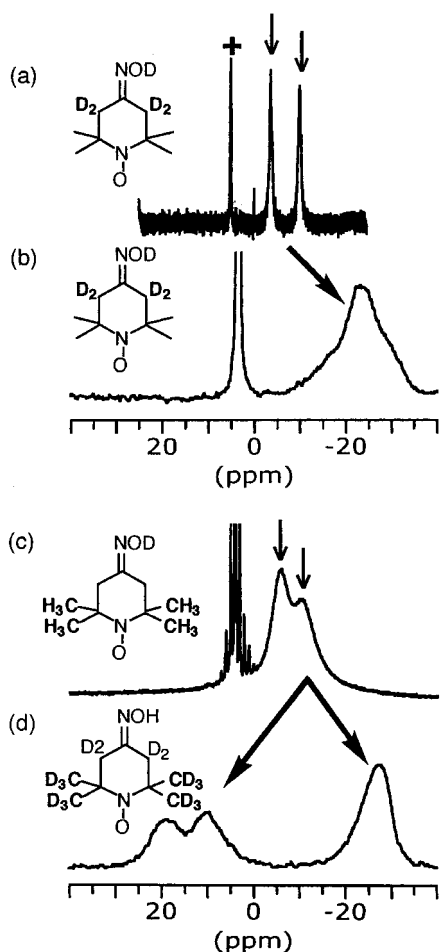


**Figure 3.** (a)  $^2\text{D}$  NMR spectrum of **3** in  $\text{CH}_3\text{OH}$  solution. The two arrows indicate methylene signals, and the plus mark (+) indicates the hydroxyl signal. The relative integrated intensity is 0.8:2.0:2.0 from a high- to low-frequency shift. (b)  $^2\text{D}$ -MAS NMR spectrum of **3** in the crystalline phase. The sharp signal near 5 ppm is due to a very small amount of  $\text{CD}_3\text{OD}$ . The integrated intensity of the solvent is very small compared to that of the methylene signal, since the solvent signal shows no spinning sideband. (c)  $^1\text{H}$  NMR spectrum of **3** in  $\text{CD}_3\text{OD}$  solution. The signal of protonated methanol dissolved in  $\text{CD}_3\text{OD}$  shows sharp signals with spinning sidebands near 3 ppm. (d)  $^2\text{D}$ -MAS NMR spectrum of **2** in the crystalline phase measured at room temperature.

X-ray structure analysis indicated that the crystallographic mirror plane runs almost through the center of the molecule, and the hydroxyl group is statically disordered into two mirror-image positions.<sup>18</sup> The molecule has no symmetry, and the unresolved signal of methylene groups shown in Figure 4a consists of several lines corresponding to the nonequivalent axial and equatorial positions of the deuteriums. Decomposition of the observed peak was difficult, and the averaged hyperfine coupling constant was determined for the methylene deuteriums from the temperature dependence of the isotropic Fermi contact shift. The temperature dependence was fitted by eqs 1 and 2 as shown in Figure 5, and the coupling constant  $A_D = -0.22$  MHz was obtained (Table 1).

For methyl groups, we found two distinct signals around 20 and  $-40$  ppm, which respectively reflected the positive and negative signs of the temperature coefficient, as shown in Figure 4b. The two signals have almost the same integrated intensity, 1.0:1.1–1.0:1.2. Although the methylene signal overlapped the methyl peak near  $-40$  ppm, this overlapping did not disturb the determination of the hyperfine coupling constants of the methyl groups, since the intensity of the methylene signal is

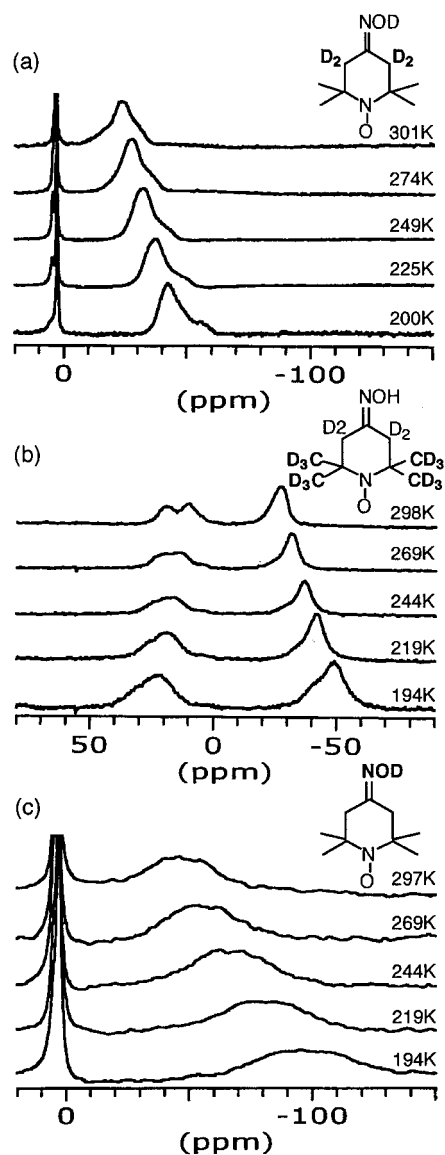


**Figure 4.** Temperature dependence of the  $^2\text{D}$ -MAS NMR spectra: (a) the methylene and hydroxyl deuterated specimen **3** (the sharp signal near 3 ppm is due to a very small amount of adsorbed  $\text{CD}_3\text{OD}$ ); (b) the methyl and methylene deuterated specimen **2**; (c) the hydroxyl deuterated specimen **4** (although the sharp signal of  $\text{CD}_3\text{OD}$  near 3 ppm looks large, its integrated intensity is very small compared to the intensity of the hydroxyl deuterium of **4** integrated over all of the spinning sidebands).

much weaker than that of the methyl group as mentioned above. Each methyl signal consists of several components. Only the signal near 20 ppm could be decomposed into two different shifts, and the shift value at the center of the signal was also estimated. The temperature dependence of these shifts was fitted by eqs 1 and 2 as shown in Figure 5, and the results are listed in Table 1. The negative hyperfine coupling constant of the methyl deuterium is comparable to that of arylimino-TEMPOs determined by  $^1\text{H}$ -MAS NMR, although the methyl and methylene signals were not resolved in the  $^1\text{H}$ -MAS NMR spectra.<sup>37</sup> The hyperfine coupling constant of deuterium can be converted to that of the proton by multiplying by the magnetogyric ratio  $\gamma_{\text{H}}/\gamma_{\text{D}}$  (see eq 4). The methyl signal with a positive hyperfine coupling constant was assigned to the axial position, and that

(37) Maruta, G.; Takeda, S.; Kawakami, T.; Mori, W.; Imachi, R.; Ishida, T.; Nogami, T.; Yamaguchi, K. *Mol. Cryst. Liq. Cryst.* **1997**, *306*, 307–314.

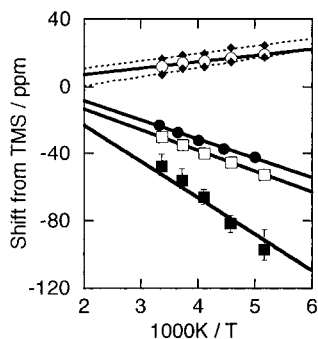


**Figure 5.** Temperature dependence of the isotropic shifts of  $^2\text{D}$ -MAS NMR of 4-hydroxyimino-TEMPO in the crystalline phase: ●, methylene deuteriums of **3**; ○, center of the signal of the axial methyl deuteriums of **2**; ◆, decomposed components of the axial methyl signal; □, equatorial methyl deuteriums of **2**; ■, hydroxyl deuterium of **4**. Since the line width of the  $^2\text{D}$ -MAS NMR signal of the hydroxyl deuterium is considerably larger than those of the other groups, the errors of the isotropic shift are also large, as shown by vertical bars. The solid lines are the result of fitting to eqs 1 and 2.

**Table 1.** Deuterium Spin Electron Spin Coupling Constant  $A_D/\text{MHz}$  of 4-Hydroxyimino-TEMPO

	experiment, <sup>a</sup> crystalline phase	BLYP [B3LYP] calculations <sup>b</sup>		
		isolated molecule	H-bonded dimer	
			H-acceptor	H-donor
<b>methylene</b>				
3-1	-0.22(1)	-0.21 [-0.25]	-0.22 [-0.26]	-0.21 [-0.25]
3-2		-0.07 [-0.10]	-0.09 [-0.13]	-0.08 [-0.11]
5-1		-0.20 [-0.24]	-0.20 [-0.25]	-0.20 [-0.24]
5-2		-0.07 [-0.10]	-0.09 [-0.13]	-0.08 [-0.10]
<b>ax-methyl 10<sup>c</sup></b>				
10-1	+0.12(1)	-0.32 [-0.37]	-0.34 [-0.40]	-0.32 [-0.37]
10-2		+0.70 [+0.53]	+0.83 [+0.66]	+0.69 [+0.53]
10-3		-0.21 [-0.23]	-0.27 [-0.28]	-0.21 [-0.23]
<b>eq-methyl 11<sup>c</sup></b>				
11-1	-0.24(1)	-0.09 [-0.11]	-0.11 [-0.13]	-0.10 [-0.11]
11-2		-0.24 [-0.30]	-0.22 [-0.28]	-0.24 [-0.30]
11-3		-0.06 [-0.09]	-0.05 [-0.10]	-0.06 [-0.09]
<b>ax-methyl 13<sup>c</sup></b>				
13-1	+0.13(2)	+0.06 [-0.02]	+0.07 [-0.01]	+0.05 [-0.02]
13-2		-0.32 [-0.37]	-0.34 [-0.40]	-0.32 [-0.37]
13-3		+0.71 [+0.54]	+0.82 [+0.66]	+0.70 [+0.54]
		-0.22 [-0.24]	-0.28 [-0.30]	-0.22 [-0.24]
<b>eq-methyl 12<sup>c</sup></b>				
12-1	-0.24(1)	-0.13 [-0.17]	-0.13 [-0.17]	-0.13 [-0.16]
12-2		-0.10 [-0.12]	-0.12 [-0.14]	-0.10 [-0.12]
12-3		-0.23 [-0.29]	-0.22 [-0.28]	-0.23 [-0.29]
12-3		-0.05 [-0.09]	-0.04 [-0.09]	-0.05 [-0.09]
hydroxyl 9-1	-0.45(10)	-0.01 [-0.01]	-0.01 [-0.01]	-0.51 [-0.73]

<sup>a</sup> The values were determined by  $^2\text{D}$ -MAS NMR. Values in parentheses are the experimental error. <sup>b</sup> The 6-31G(d,p) basis set was used. Values in brackets were calculated by B3LYP. The molecular geometry was taken from the crystal structure, except for the hydroxyl hydrogen atoms. The geometry of the hydroxyl hydrogen atoms was optimized by the PM3 method. Calculations were performed for the isolated doublet molecule and for the hydrogen-bonded triplet dimer, which consists of a proton acceptor and a proton donor. <sup>c</sup> Averaged value of three hydrogen atoms for the computed coupling constants. When we took a shift value for the center of the signal of axial methyl groups, a hyperfine coupling constant of +0.07 MHz was obtained.

with a negative hyperfine coupling constant was assigned to the equatorial position on the basis of BLYP and B3LYP calculations for the hyperfine coupling constants. The results of the calculations are summarized in Table 1, and the numbering scheme for the hydrogen atoms is shown in Figure 6. The BLYP and B3LYP calculations predict that all of the hydrogen atoms of the equatorial methyl and methylene groups exhibit negative coupling constants, which are predominantly induced by the spin polarization effect within a molecule. On

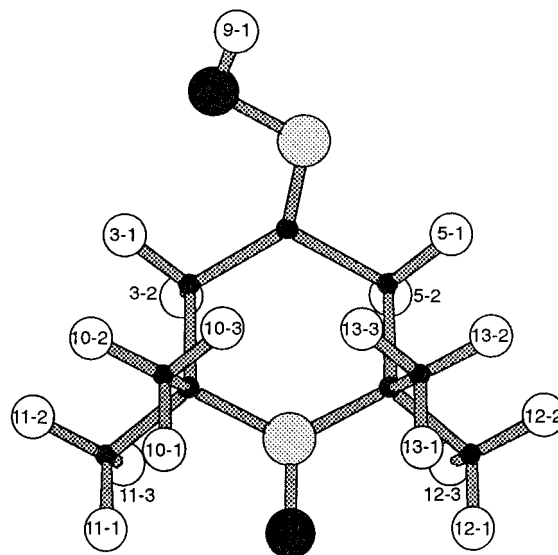


**Figure 6.** Numbering scheme for the hydrogen atoms of 4-hydroxyimino-TEMPO.

the other hand, one of the three hydrogen atoms of the axial methyl group, e.g., 13-2 in Figure 6, bears a large positive coupling constant +0.71 MHz (+0.54 MHz), while two others exhibit negative values: -0.32 and -0.22 MHz (-0.37 and -0.24 MHz). The values in parentheses are the results of B3LYP calculations. A negative coupling constant is induced by a spin polarization mechanism, and a positive value is brought about by hyperconjugation in a molecule. An unpaired electron localized on the N-O radical site induces an electron spin density wave by the spin polarization effect. The sign of the spin density at each position alternates through successive bonds as O-N( $\uparrow$ )-C $_{\alpha}$ ( $\downarrow$ )-C $_{\beta}$ ( $\uparrow$ )-D $_{\beta}$ ( $\downarrow$ ). This mechanism makes the coupling constant of axial CD $_3$  deuteriums negative. The effect of hyperconjugation exceeds that of spin polarization at deuterium positions 10-2 and 13-2 and gives a positive spin density at these deuterium positions of the axial methyl groups. The  $\pi^*$  orbital of the N-O radical group may be delocalized by hyperconjugation, and SOMO may extend to one of the deuteriums of each axial methyl group (10-2 and 13-2). Fast rotation of the methyl group, which means rapid exchange of deuterium over the three positions, effectively averages the positive and negative hyperfine coupling constants. Thus, small positive values (+0.12 and +0.13 MHz) were observed for the two axial methyl groups. The observed positive coupling constant is concrete evidence of the extension of SOMO to the axial methyl groups of 4-hydroxyimino-TEMPO in the crystalline phase. A similar positive hyperfine coupling constant of the axial methyl proton was noted for TEMPO and TEMPOL.<sup>35</sup> Interestingly, the isotropic shift of the methyl protons of **3** appeared at -6 and -10 ppm in methanol solution at 300 K (Figure 3c), indicating that the averaged hyperfine coupling constants of all of the methyl groups are negative. This experimental result indicates that the effect of hyperconjugation disappeared in methanol solution and is very sensitive to the change in the molecular conformation in different phases. This point is important for the discussion below of intermolecular magnetic interaction through methyl groups in organic magnetic solids.

The shift of the hydroxyl deuterium changed dramatically when the temperature was lowered, as shown in Figure 4c, and a large negative hyperfine coupling constant (-0.45 MHz) was deduced from eqs 1 and 2 (Figure 5 and Table 1). Since the width of the signal of the hydroxyl group is much greater than

**Table 2.** Calculated Effective Exchange Integrals  $J/\text{cm}^{-1}$  of 4-Hydroxyimino-TEMPO

	BLYP <sup>a</sup>	B3LYP <sup>a</sup>	INDO	expt <sup>b</sup>
hydrogen-bonded pair	+0.06	+0.07	+0.04	
methyl-contacted pair	-0.23	+0.30	+0.07	
one-dimensional Heisenberg chain				+0.44

<sup>a</sup> The 6-31G(d,p) basis set was used. <sup>b</sup> Reference 16.

those of other signals described above, the error of the shift value is large, as indicated by horizontal bars in Figure 5. The BLYP and B3LYP calculations gave a small negative coupling constant of  $-0.01$  MHz for an isolated molecule. On the other hand, these calculations for hydrogen-bonded molecules, which are linked by contact I as shown in Figure 1, gave large negative coupling constants of  $-0.51$  and  $-0.73$  MHz for hydrogen-bonded deuterium. The calculated values are comparable to the observed value, indicating that the large electron spin density on the hydroxyl deuterium is induced by the N–O radical group of the neighboring molecule through hydrogen bonding. The minus sign of the electron spin density induced by the intramolecular coupling is in phase with the sign of the intramolecular spin polarization network.

The diamagnetic shift of the hydroxyl deuterium estimated from eq 1 is 20 ppm. This value is outside the normal range for diamagnetic compounds. Since the electronic state of the hydrogen acceptor, i.e., the N–O radical group, is different from that of the corresponding closed-shell molecule, the diamagnetic chemical shift of the hydroxyl deuterium linked to the N–O radical group through hydrogen bonding is not necessarily the same as that in closed-shell systems.

**Magnetic Interaction in 4-Hydroxyimino-TEMPO in the Crystalline Phase.** From the viewpoint of the crystal structure of 4-hydroxyimino-TEMPO, there are two kinds of close contacts between neighboring molecules in the crystalline phase, i.e., hydrogen bonding to form an infinite chain (contact I in Figure 1) and contact between axial methyl hydrogens and a neighboring N–O radical group to form a zigzag chain (contact II). We concentrate here on the hyperfine coupling constants of the hydroxyl deuterium and the axial methyl deuterium. The large negative hyperfine coupling constant of the hydrogen-bonded hydroxyl deuterium was almost reproduced by BLYP and B3LYP calculations for a hydrogen-bonded dimer model. The intermolecular magnetic interaction, i.e., the effective exchange integral  $J$ , can be estimated by BLYP and B3LYP calculations. The BLYP calculation is known to slightly underestimate electron spin density distributions, whereas the semiempirical INDO calculation often overestimates them and gives reasonable effective exchange integrals  $J$ .<sup>27</sup> The B3LYP method falls between the BLYP and INDO calculations. The three calculation methods were used to estimate the effective exchange integrals for the two kinds of dimer models, i.e., contact I and contact II in Figure 1. The results of the calculations and the experimental value deduced from a measurement of the magnetic susceptibility by assuming a one-dimensional ferromagnetic Heisenberg model<sup>16</sup> are summarized in Table 2. All three calculation methods indicated ferromagnetic interaction (positive value of  $J$ ) for the hydrogen-bonded dimer. The sign of the electron spin density of the hydroxyl hydrogen induced by an adjacent N–O radical group bearing a positive spin is in phase with the intramolecular spin alternation, which is polarized by the positive spin of the N–O radical group on the same molecule. Thus, hydrogen bonding contributes to the intermolecular magnetic interaction as a ferromagnetic coupler in the crystalline phase of 4-hydroxyimino-TEMPO.

For the axial methyl-contacted dimer, the BLYP calculation showed antiferromagnetic interaction (negative value of  $J$ ) due to an underestimation of the spin polarizations, whereas the INDO and B3LYP calculations indicated ferromagnetic interaction as shown in Table 2. These calculations suggest that the magnetic interaction through the axial methyl hydrogens is somewhat delicate, which is compatible with a conflict between the two mechanisms for polarizing the electron spins in opposite directions. The axial methyl hydrogens 10-3 and 13-3 depicted in Figure 6 are located closest to an adjacent N–O radical group. The distances are 0.247 and 0.277 nm.<sup>18</sup> These hydrogens bear the negative spin density predominantly induced by the spin polarization within a molecule and can contribute to ferromagnetic intermolecular interaction, which is ferromagnetic indirect interaction. Axial methyl hydrogens 10-2 and 13-2 bearing a positive spin density are located far from the adjacent N–O radical group (0.358 and 0.417 nm) compared to hydrogens 10-3 and 13-3. Hyperconjugation, i.e., the spread of a SOMO, is sensitive to changes in conformation and in the orientation of the axial methyl group. The SOMO spread by hyperconjugation can interact both antiferromagnetically and ferromagnetically with that of a neighboring molecule, which comes from direct SOMO–SOMO interaction with and without overlapping, respectively. This effect suggests that intermolecular magnetic interaction through the axial methyl group may account for the changes in both the ferromagnetic and antiferromagnetic interactions with a slight change in the molecular arrangements in the crystal.

In the crystalline phase of 4-hydroxyimino-TEMPO, in addition to the ferromagnetic interaction via hydrogen bonding (contact I in Figure 1) within an infinite molecular chain, the axial methyl contact may also mediate ferromagnetic interaction between the two ferromagnetic hydrogen-bonded chains to form a double chain, as shown in Figure 1.

Along the crystallographic  $b$  axis, which is perpendicular to the hydrogen-bonded chains, an axial methylene hydrogen is located close (0.27 nm) to the hydroxyl oxygen of the neighboring hydrogen-bonded chain. Molecular orbital calculations showed that a positive electron spin density of the hydroxyl oxygen induced by intramolecular spin polarization is largely enhanced by hydrogen bonding with the neighboring N–O radical group in the same chain. The axial methylene hydrogen bearing a negative electron spin density can interact ferromagnetically with the positive electron spin density of the hydroxyl oxygen. The interaction between double chains along the crystallographic  $b$  axis can also be ferromagnetic, although such interaction is likely weak. More weak contacts are seen between the axial methyl hydrogen bearing a positive electron spin density due to hyperconjugation and equatorial methyl hydrogens bearing a negative electron spin density along the crystallographic  $a$  axis. These distances are 0.29–0.30 nm. The BLYP and B3LYP calculations for the methyl-contacted dimer indicated that the negative electron spin density of the equatorial methyl hydrogens is significantly enhanced. This effect may contribute to the intermolecular ferromagnetic interactions along the  $a$  axis.

## 6. Conclusion

In this paper, we investigated the mechanism of intermolecular magnetic interaction in an organic magnetic crystal of 4-hydroxyimino-TEMPO, which exhibits a ferromagnetic phase transition at low temperature. A large negative electron spin density was found at the deuterium atom of the hydrogen-bonded hydroxyl group of partially deuterated 4-hydroxyimino-TEMPO

in the crystalline phase by high-speed magic angle spinning  $^2\text{D}$  NMR. The large negative electron spin density is induced by the N–O radical group of the neighboring molecule through hydrogen bonding and mediates the intermolecular ferromagnetic interaction within the hydrogen-bonded chain. A small positive hyperfine coupling constant was observed for the axial methyl hydrogens, showing that the positive and negative values of each hydrogen atom were effectively averaged by rapid rotation of the methyl group at high temperature. One of the axial methyl hydrogens bearing a negative spin density establishes ferromagnetic contact with the N–O radical group of a neighboring chain. Generally, the axial methyl group may contribute to both the ferromagnetic and antiferromagnetic interactions with a slight change in the orientation and conformation of the methyl group, due to the presence of two different mechanisms, i.e., ferromagnetic indirect interaction assisted by spin polarization, and ferro- or antiferromagnetic direct interac-

tion between the SOMO that is spread on the methyl group by hyperconjugation and the SOMO of the neighboring molecule. The high-speed magic angle spinning deuterium NMR method is very useful for investigating the local magnetic structure in the crystalline phase and the mechanism of intermolecular magnetic interactions at a microscopic level.

**Acknowledgment.** This research was supported by grant-in-aid for Scientific Research on Basic Science (No. 09640681) and on Priority Areas (A) "Creation of Delocalized Electronic Systems" (No. 10146212) from the Ministry of Education, Science, Culture and Sports of Japan. S.T. is grateful to the Iketani Science and Technology Foundation for a financial support. G.M. thanks the Japan Society for the Promotion of Science for Young Scientists for a Research Fellowship.

JA982393W